Anal. Chem. **2006,** *78,* 2314−2318

Hybridization Probe for Femtomolar Quantification of Selected Nucleic Acid Sequences on a Disposable Electrode

Daniel M. Jenkins,*,† Bilal Chami,† Matthias Kreuzer,‡ Gernot Presting,† Anne M. Alvarez,§ and Bor Yann Liaw||

Molecular Biosciences and Bioengineering, Plant and Environmental Protection Sciences, and Hawaii Natural Energy Institute, University of Hawaii, Honolulu, Hawaii 96822 and Technische Universität München, München, Germany

Mixed monolayers of electroactive hybridization probes on gold surfaces of a disposable electrode were investigated as a technology for simple, sensitive, selective, and rapid gene identification. Hybridization to the ferrocene-labeled hairpin probes reproducibly diminished cyclic redox currents, presumably due to a displacement of the label from the electrode. Observed peak current densities were roughly 1000× greater than those observed in previous studies, such that results could easily be interpreted without the use of algorithms to correct for background polarization currents. Probes were sensitive to hybridization with a number of oligonucleotide sequences with varying homology, but target oligonucleotides could be distinguished from competing nontarget sequences based on unique "melting" profiles from the probe. Detection limits were demonstrated down to nearly 100 fM, which may be low enough to identify certain genetic conditions or infections without amplification. This technology has rich potential for use in field devices for gene identification as well as in gene microarrays.

Emerging technologies for rapid detection of specific nucleic acid sequences have important implications in a variety of fields from clinical medicine to experimental biology and management of disease epidemics. For example, immunodiagnostic strips for the wilt-inducing bacterium *Ralstonia solanacearum* are not able to distinguish cells of the select agent race 3 biovar 2 from more ubiquitous strains,[1] whereas these strains may be differentiated based on genetic differences. The race 3 biovar 2 strains of the pathogen cause global damage to potato crops in excess of $950 million annually, yet so far have not been introduced to potato-producing regions in North America.[2]

Traditionally, most methods for identifying and quantifying genetic sequences involve optical transduction mechanisms. These include the use of intercalating dyes such as ethidium bromide[3] or Picogreen,[4,5] hybridization to fluorescently or otherwise optically labeled probes,[6] and mechanisms of quenched fluorescence such as Molecular Beacons[7−9] or nuclease-activated probes.[10,11] These optical probes form the basis of real-time PCR methods, which have revolutionized the laboratory identification of organisms and gene-related biological conditions. In addition, many research groups are actively engaged in developing field instrumentation based on optical detection of specific nucleic acid sequences.[12]

Despite the versatility and advances made with optical methods for nucleic acid detection, there is reason to believe that electrochemical methods may ultimately be preferable for distributed use in the field or even in microarray applications. The most widely used and commercially successful biosensor is the disposable electrochemical glucose test strip, which is notable for its simplicity and low cost.[13] This is based on the low cost of screen-printing technologies for producing the electrodes and the simplicity of the instrument used to read the strips. Commercial versions of the reader retail for prices in the vicinity of $30, making the technology accessible for distributed use in the large home health care market.

Recent advances in the electrochemical detection of nucleic acids portend a similar revolution for gene-based sensors. A number of formats for electrochemical detection are described in the literature, including hybridization with probes conjugated to a redox-active label[14] or a redox-mediating enzyme.[14,15] The use

* To whom correspondence should be addressed. E-mail: danielje@hawaii.edu. Phone: (808) 956-6069. Fax: (808) 956-3542.

† Molecular Biosciences and Bioengineering, University of Hawaii.

‡ Technische Universität München.

§ Plant and Environmental Protection Sciences, University of Hawaii.

|| Hawaii Natural Energy Institute, University of Hawaii.

(1) Alvarez, A. M.; Berestecky, J.; Stiles, J. I.; Ferreira, S. A.; Benedict, A. A., Koahsiung, Taiwan 1992; ACIAR.

(2) APHIS-PPQ. *PPQ Pest Detection and Management Programs*; Aphis, U., Ed.; 2004.

(3) Kuroiwa, T.; Suzuki, T.; Kawano, S. *Cell Struct. Funct.* **1979**, *4*, 399−399.

(4) Wu, J.; Delwiche, M.; Cullor, J.; Smith, W., Ottawa, Canada, 2004; ASAE Paper 04-7040.

(5) Kral, T.; Widerak, K.; Langner, M.; Hof, M. *J. Fluoresc.* **2005**, *15*, 179−183.

(6) Vandekken, H.; Hagenbeek, A.; Bauman, J. G. J. *Leukemia* **1989**, *3*, 724−728.

(7) Matsuo, T. *Biochim. Biophys. Acta: General Subjects* **1998**, *1379*, 178−184.

(8) Fang, X. H.; Li, J. W. J.; Perlette, J.; Tan, W. H.; Wang, K. M. *Anal. Chem.* **2000**, *72*, 747A−753A.

(9) Roy, S.; Kabir, M.; Mondal, D.; Ali, I. K. M.; Petri, W. A.; Haque, R. *J. Clin. Microbiol.* **2005**, *43*, 2168−2172.

(10) Schoen, C. D.; Knorr, D.; Leone, G. *Phytopathology* **1996**, *86*, 993−999.

(11) He, J. W.; Jiang, S. *Appl. Environ. Microbiol.* **2005**, *71*, 2250−2255.

(12) Sandia; Sandia National Labs: Albuquerque, NM, 2005; SAND 2005−1593P.

(13) Kissinger, P. T. *Biosens. Bioelectron.* **2005**, *20*, 2512−2516.

(14) Kerman, K.; Kobayashi, M.; Tamiya, E. *Measure. Sci. Technol.* **2004**, *15*, R1−R11.

(15) Mir, M.; Katakis, I. *Anal. Bioanal. Chem.* **2005**, *381*, 1033−1035.

10.1021/ac051619s CCC: $33.50
Published on Web 02/24/2006

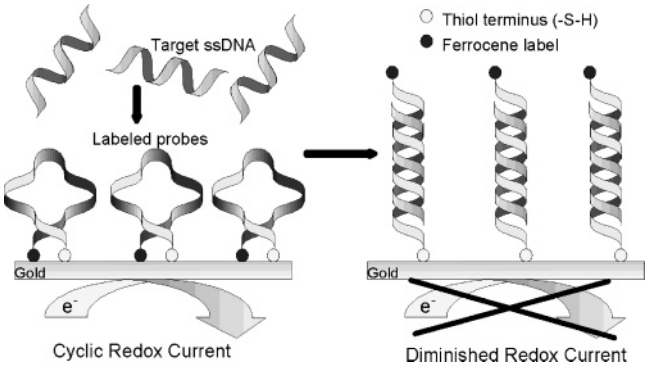

Figure 1. Label-free electrochemical detection of nucleic acid hybridization. Target ssDNA hybridizes to a complementary region of a hairpin probe labeled with ferrocene, inducing a conformational change in the probe, which displaces the ferrocene from the electrode, effectively diminishing peak redox currents measured by cyclic voltammetry.

of screen-printed electrodes for electrochemical detection of enzyme mediators captured during hybridization reactions has recently been reported,[16] and instruments using this technology are available commercially (e.g., AndCare 100, Alderon Biosciences, Durham, NC; http://www.alderonbiosciences.com/instruments.html). Compared to optical transduction mechanisms, electrochemical methods for nucleic acid detection are significantly simpler and less expensive, are not sensitive to the precision of the alignment of the sample and optical components, can be made in a format similar to immunostrip tests, which are widely used in field diagnostics, and use less hazardous reagents, which are more easily contained on a solid phase.

A promising development for label-free electrochemical biosensors for DNA is the use of self-complementary probe sequences, which form hairpin loops on the electrode surface. These have been used to screen for DNA ligase activity[17] and for the direct detection of complementary DNA sequences.[18−21] In principle, these sensors work like molecular beacons—hybridization to the target disrupts the self-hybridization of the probe, causing it to undergo a conformational change (Figure 1), which displaces a redox-active label (e.g., ferrocene) from the electrode surface. This results in a diminished efficiency for electron transfer to the label, which can be detected as a drop in peak redox current measured by cyclic voltammetry. The advantage of this method over other electrochemical methods is that hybridization is measured directly, obviating the need for a labeling or substrate addition step.

In this article, we report on efforts to improve the detection limit and selectivity of electrochemical hairpin probes by immobilizing them onto disposable screen-printed electrodes. As a model, we have used probes with sequences complementary to DNA specific to *Agrobacterium tumefaciens* strain C58, a bacterium commonly used for plant gene transformation.[22] Disarmed versions of the bacteria are commercially available and may be handled safely in the laboratory without danger of accidentally introducing genetic modifications into the environment.

EXPERIMENTAL SECTION

Structure of Oligonucleotides. Probe oligonucleotides, functionalized with a three-carbon alkanethiol at the 3′ end and with ferrocenemonocarboxylic acid conjugated through an amide linkage at the 5′ end, were purchased from a commercial DNA synthesizer (Genemed Synthesis, Inc., South San Francisco, CA). Two probes were designed to be complementary to the same 24-base target oligonucleotide representing a sequence specific to *A. tumefaciens* C58. The probes differed only in the length of the self-complementary fragment (Table 1), with identical loop portions complementary to the same target. To test specificity, two nonspecific 24-base oligonucleotides were also tested: one (PSC) that had some complementarity with the stems of the probes and another (SNM) that differed from the target DNA by a single-nucleotide mismatch (Table 1). All nonprobe oligonucleotides were obtained commercially (Integrated DNA Technologies, Coralville, IA).

Application of software for nucleic acid folding prediction (Mfold)[23] verified that the most thermodynamically stable foldings for both probes resulted in self-hybridized stem−loop structures, with terminal nucleotides of the probes pairing with each other as suggested in Figure 1. The "stem" refers to the hybridized fragment contiguous with the terminal nucleotides.

Preparation of Electrodes. Disposable screen-printed electrodes were purchased commercially (type AC1.W1.R2, BVT Technologies, Brno, Czech Republic). Each electrode was printed on a corundum ceramic material, with working and counter electrodes patterned in gold and a silver reference electrode coated in silver chloride. Working electrodes were 1-mm diameter. To immobilize probe DNA onto the working electrode, a 2-μL droplet of 2.5 μM solution of probe DNA in 1 M $NaClO_4$ was applied at room temperature (22 °C) and allowed to evaporate. After 45 min, a second 2-μL droplet of the same solution was applied for another 45 min, after which it was rinsed off with 1 M $NaClO_4$ solution. The thiol modification of the probe DNA allowed it to adhere to the gold in a monolayer.[16,24−26] After probe immobilization, a 2-μL droplet of 10 mM β-mercaptoethanol in 1 M $NaClO_4$ was applied to the working electrode for 5 min, which was then rinsed off and stored in 1 M $NaClO_4$. All solutions used in this research contained $NaClO_4$ to inhibit the decomposition of the oxidized state of the ferrocene derivative.[27] The β-mercaptoethanol was used to fill any gaps in the monolayer, forcing the immobilized DNA to align reproducibly in an orientation extending away from the electrode surface (Figure 2).[24,25]

(16) Carpini, G.; Lucarelli, F.; Marrazza, G.; Mascini, M. *Biosens. Bioelectron.* **2004**, *20*, 167−175.
(17) Zauner, G.; Wang, Y. T.; Lavesa-Curto, M.; MacDonald, A.; Mayes, A. G.; Bowater, R. P.; Butt, J. N. *Analyst* **2005**, *130*, 345−349.
(18) Fan, C. H.; Plaxco, K. W.; Heeger, A. J. *Proc. Natl. Acad. Sci.. U.S.A.* **2003**, *100*, 9134−9137.
(19) Mao, Y. D.; Luo, C. X.; Ouyang, Q. *Nucleic Acids Res.* **2003**, *31*, e108.
(20) Immoos, C. E.; Lee, S. J.; Grinstaff, M. W. *Chembiochem* **2004**, *5*, 1100−1103.
(21) Fan, C. H.; Plaxco, K. W.; Heeger, A. J. *Trends Biotechnol.* **2005**, *23*, 186−192.
(22) Broothaerts, W.; Mitchell, H. J.; Weir, B.; Kaines, S.; Smith, L. M. A.; Yang, W.; Mayer, J. E.; Roa-Rodriguez, C.; Jefferson, R. A. *Nature* **2005**, *433*, 629−633.
(23) Zuker, M. *Nucleic Acids Res.* **2003**, *31*, 3406−3415.
(24) Herne, T. M.; Tarlov, M. J. *J. Am. Chem. Soc.* **1997**, *119*, 8916−8920.
(25) Levicky, R.; Herne, T. M.; Tarlov, M. J.; Satija, S. K. *J. Am. Chem. Soc.* **1998**, *120*, 9787−9792.
(26) Liang, T. T.; Azehara, H.; Ishida, T.; Mizutani, W.; Tokumoto, H. *Synth. Met.* **2004**, *140*, 139−149.
(27) Han, S. W.; Seo, H.; Chung, Y. K.; Kim, K. *Langmuir* **2000**, *16*, 9493−9500.

Table 1. Oligonucleotide Sequences Used in Experiments[a]

probes	
1	5′ Fc[b]-CCTGC**CGACCCGGCCGTTGATCGTCGGTC**GCAGG-SH[c] 3′
2	5′ Fc[b]-CGACGCCTGC**CGACCCGGCCGTTGATCGTCGGTC**GCAGGCGTCG-SH[c] 3′
hybridization targets	
target	3′ **GCTGGGCCGGCAACTAGCAGCCAG** 5′
single-nucleotide mismatch (SNM)	3′ **GCT**T**GGCCGGCAACTAGCAGCCAG** 5′
partial stem complement (PSC)	3′ GGTCGGGGCTTCTCCAACGCGACC 5′

[a] Underlined nucleotides are self-complementary (stem) segments of probe, and boldface nucleotides are complementary to target/probe. [b] Fc represents conjugation to ferrocene. [c] SH represents thiol functionalization.

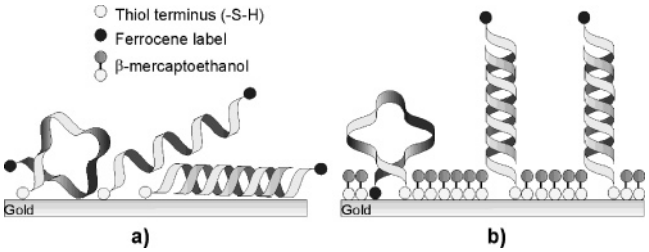

Figure 2. (a) Unpredictable alignment and orientation of thiol-functionalized oligonucleotides immobilized onto gold without β-mercaptoethanol spacers. (b) After application of β-mercaptoethanol spacer molecules, immobilized oligonucleotides reproducibly align in an orientation extending away from the electrode surface.[24,25]

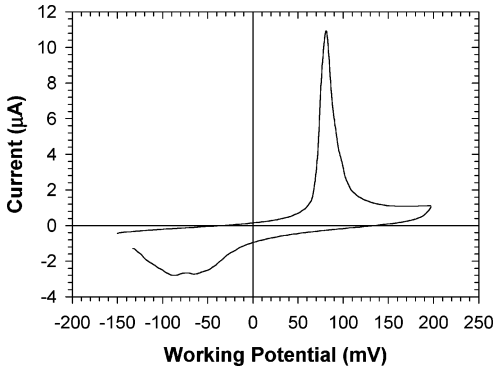

Figure 3. Voltammogram of a representative probe 2 electrode in the absence of DNA (peak oxidation current 11.0 μA).

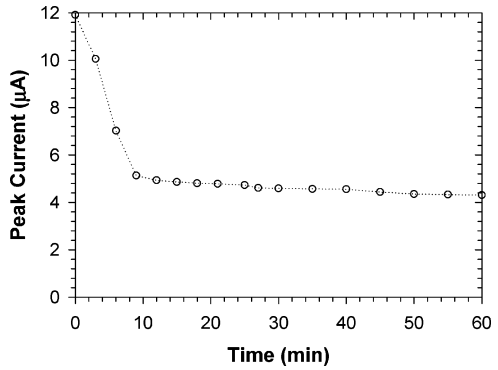

Figure 4. Peak oxidation currents measured on a probe 1 electrode during incubation with 10 nM target DNA.

Hybridization Reactions. Hybridization reactions were carried out at room temperature (22 °C) in standardized target oligonucleotide solutions. These were made by dissolving oligonucleotides in a solution of 1 M $NaClO_4$ and 0.1 M KCl, after discarding any precipitated potassium perchlorate. Electrodes were incubated in 0.8 mL of these standard solutions (typically for 60 min unless specified otherwise) and then analyzed by cyclic voltammetry.

Cyclic Voltammetry. Cyclic voltammetry measurements were recorded with a commercial potentiostat (Omni 101, Cypress Systems, Saint Louis, MO) using the hybridization solution as electrolyte. Potentials relative to the Ag/AgCl reference electrode were scanned at 100 mV/s once from −150 to +200 mV and back, recording the peak oxidation current for ferrocene occurring near 80 mV. For convention, an oxidation current or stripping of electrons from the probe was denoted as a positive current.

Hybridization Product Melting Curves. To resolve target hybridization from interfering nonspecific hybridizations, electrodes were heated in the hybridization solutions to try to discern the melting temperatures. Heating to near 100 °C was achieved in ∼30 min by immersion of the centrifuge tubes into a water bath on a hot plate. Temperature was recorded with a type K thermocouple, and peak oxidation currents were recorded at intervals of 1−3 °C.

RESULTS AND DISCUSSION

A typical voltammogram of an electrode with immobilized probe 2 in the absence of DNA (Figure 3) shows a strong oxidation peak at ∼80 mV relative to the Ag/AgCl reference electrode, with a corresponding broader and flatter reduction peak centered near −70 mV. These peaks are more distinctive and ∼1000× larger than peaks observed using conventional electrodes of similar size.[18,20] These discrepancies cannot be explained on the basis of the surface morphology of the screen-printed electrodes based on unpublished SEM images. The peaks observed in this research are also shifted in potential compared to previous observations for the oxidation of conjugated ferrocene,[18,20] which may be at least partly explained by the low chloride ion concentration used in the electrolyte in these experiments compared to the chloride ion concentration in a standard Ag/AgCl electrode, thus favoring oxidation at the working electrode at a lower potential.

Numerical integration of the oxidation current from Figure 3 indicates a net charge transfer of ∼25 pmol of electrons. This contrasts by ∼3 orders of magnitude from predictions assuming single electron transfer to each ferrocene label and considering that surface densities for DNA immobilization using similar chemistries[28] are typically in the vicinity of 0.05 pmol mm^{-2}. This discrepancy is especially odd considering that only 10 pmol of

(28) Moses, S.; Brewer, S. H.; Lowe, L. B.; Lappi, S. E.; Gilvey, L. B. G.; Sauthier, M.; Tenent, R. C.; Feldheim, D. L.; Franzen, S. *Langmuir* **2004**, *20*, 11134−11140.

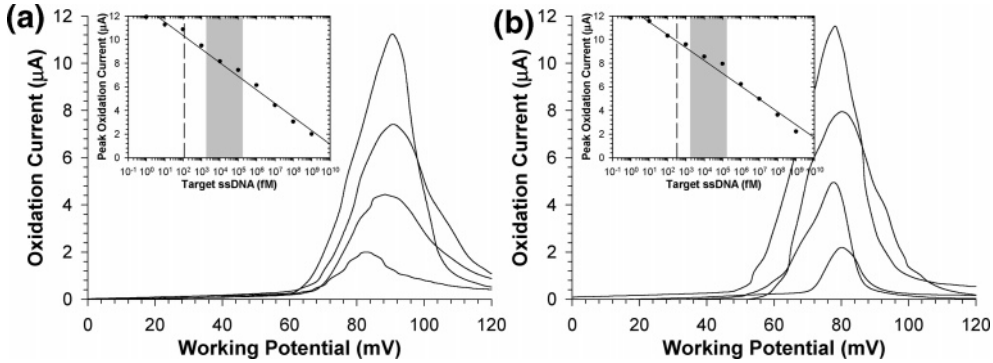

Figure 5. Oxidation current scans and standard curves (insets) for (a) probe 1 electrodes and (b) probe 2 electrodes. Current scans, in order of diminishing peaks, are for probes incubated in the absence of DNA and incubated for 60 min in 100 pM, 10 nM, and 1 μM target ssDNA sequence. The dashed lines in insets represent the detection limits for the respective probes, and the shaded regions represent the quantity of bacterial DNA commonly found in the vascular tissue of plants symptomatic of bacterial wilt,[29] assuming one gene copy per cfu. Calibration data for probe 1, $I = 12.6 - 1.15$ log[DNA], $R^2 = 0.985$, standard error 0.45 μA, detection limit 115 fM; for probe 2, $I = 12.6 - 1.08$ log[DNA], $R^2 = 0.981$, standard error 0.48 μA, detection limit 330 fM.

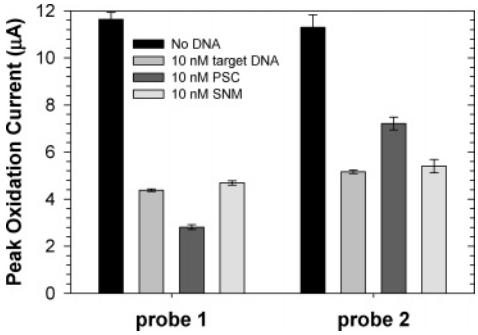

Figure 6. Observed peak currents for electrodes in the absence of DNA and after incubation with 10 nM of target, single-nucleotide mismatch (SNM), and partial stem complement (PSC) DNA fragments. Error bars show a single standard error.

probe DNA was applied to the electrode in the initial immobilization step. However, similar discrepancies can be observed in data from previous studies using a similar detection mechanism.[18,19]

Successive scans of a probe 1 electrode during incubation with 10 nM target oligonucleotide (Figure 4) indicate that the binding reaction in this case reaches ~90% of the change to equilibrium within 10 min. These data also indicate that incubation with the target for 30 min is enough to reach an approximate equilibrium.

Current scans for probe 1 and probe 2 electrodes (Figure 5) demonstrate a consistent drop in oxidation current peak for all target DNA concentrations tested from 1 fM to 1 μM. These data show that the target DNA can be quantified over ~9 orders of magnitude using a logarithmic regression. Due to the high current peaks observed in these electrodes, good results could be obtained without using algorithms to correct for the background polarization current. This greatly reduces the processing requirements for a practical instrument based on this design. Detection limits, estimated as the amount of DNA corresponding to a drop in the peak current of three standard errors from the average peak current observed in the absence of DNA, were observed to be 115 and 330 fM for probes 1 and 2, respectively. These correspond to absolute detection limits of 90 and 260 amol and are low enough to directly detect unamplified bacterial DNA typically found in vascular tissue of plants symptomatic of bacterial wilt,[29] assuming one gene copy per cfu.

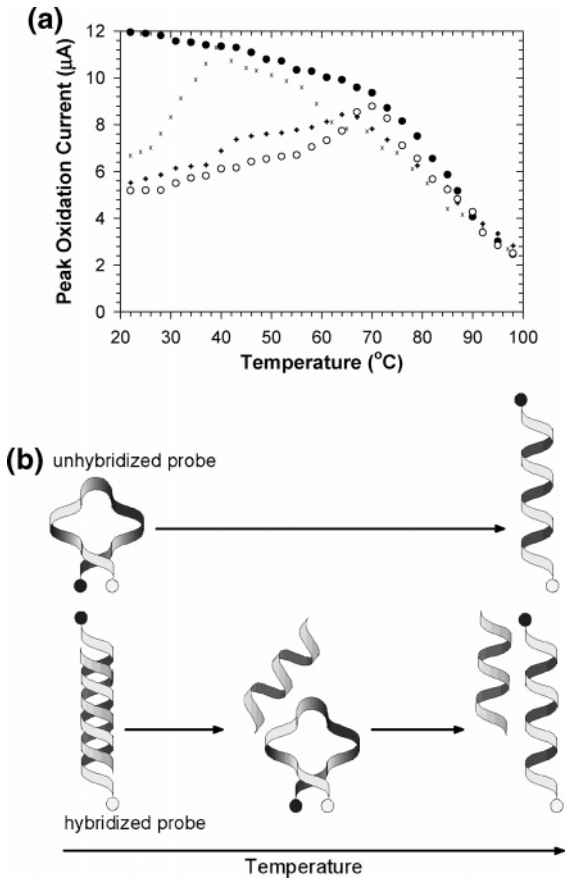

Figure 7. (a) Melting curves for probe 2 in the absence of DNA (●), hybridized in 10 nM perfect complement oligonucleotide (○), hybridized in 10 nM single-nucleotide mismatch oligonucleotide (+), and hybridized in 10 nM partial stem complement oligonucleotide (×). (b) Hypothetical temperature-induced transitions in probe conformation for unhybridized and hybridized probe molecules.

Comparison of peak oxidation currents observed in the absence of DNA to those after incubation with 10 nM of the different oligonucleotides (Figure 6) shows that each sequence is reactive with each probe. These nonspecific effects are due to similarity to the "target" sequence in the case of the single-nucleotide

(29) Swanson, J. K.; Yao, J.; Tans-Kersten, J.; Allen, C. *Phytopathology* **2005**, *95*, 136−143.

Table 2. Predicted Thermodynamic Parameters and Melting Temperatures of Probes in Stem−Loop Conformation ("Self-Pairing") or Hybridized to Various Oligonucleotide Sequences (from RNAsoft[32])

hybridization product		ΔG^a	ΔH^a	ΔS^b	$T_m{}^c$
probe 1 pairings	self-pairing	−116	−776	−2.24	45.6
	target oligo	−187	−872	−2.32	79.5
	SNM oligo	−163	−779	−2.09	74.8
	PSC oligo	−69	−578	−1.73	34.2
probe 2 pairings	self-pairing	−209	−1174	−3.27	65.6
	target oligo	−187	−872	−2.32	79.5
	SNM oligo	−163	−779	−2.09	74.8
	PSC oligo	−116	−777	−2.24	51.1

[a] Unit: kJ mol^{-1}. [b] Unit: kJ mol^{-1} K^{-1}. [c] Melting temperature: °C.

mismatch (SNM) and may be due to complementarity with the stem region of the probe for the partial stem complement (PSC). The terminals of the PSC fragment are complementary to four of the five nucleotides in the stem of probe 1 (Table 1), and the reactivity of this sequence compared to the target suggests that the hairpin probes are particularly susceptible to disruption from binding in the stem region. By comparison, probe 2 has a lower affinity for the PSC fragment, as the complementarity is with only 4 of the 10 nucleotides in the stem (Table 1). These results are consistent with previous thermodynamic studies of hairpin molecular beacons with "shared stem" complementarity to the target.[30]

To distinguish nonspecific interfering sequences from the actual target sequence, the electroactivity of the probes can be monitored as a function of temperature. In studies with molecular beacons, melting of nonspecific DNA fragments from the probe at temperatures lower than the melting temperature of the probe target provides a means of discriminating nonspecific binding from a true match.[31] We have observed an analogous effect using electroactive hairpin probes. Melting of nonspecific fragments from probe 2 allows the probe to reform a hairpin structure, causing the peak currents to occur at lower temperatures than those observed for the target DNA (Figure 7). The target sequence could be readily distinguished from a single-nucleotide mismatch by a melting temperature difference of ~5 °C. The stem-interfering fragment (PSC) was observed to melt from the probe at an even lower temperature, as was expected due to the low degree of homology between the sequences.

The observed reactivities of the assorted oligonucleotides with the probe, as well as their melting behaviors, can be partially explained by the thermodynamic stabilities predicted for the pairings using software tools available on the Internet (RNAsoft).[32] A summary of these simulations (Table 2) indicates that the self-hybridized conformation of probe 2 is more stable than the analogous conformation of probe 1, which can help explain the slightly higher detection limit using this probe. In addition, these simulations predict substantial differences in melting temperatures for the different complexes, supporting the use of temperature control to discriminate nonspecific binding effects from the target. Fabrication of electrode arrays with on board heaters[33−35] may allow rapid and energy-efficient thermal processes to improve the specificity of these types of sensors, which may make this technology especially attractive for field applications.

CONCLUSIONS

Due to its simplicity, the basic principle used in these experiments was identified as being appropriate for the development of an instrument for field gene identification. In our work, we have demonstrated a greater level of sensitivity than has been shown before using this technology. We have further demonstrated that melting curves can be used to distinguish hybridization to target oligonucleotides from competing sequences down to a single-nucleotide mismatch. Large peak currents could be easily discriminated without correction from background polarization currents, thereby simplifying data analysis and greatly reducing the processing power required for a field instrument or gene array. If coupled with isothermal gene amplification techniques, the technology may be an inexpensive and powerful tool for the rapid and selective detection of biological agents in the field. The technology is also promising as an alternative for inexpensive gene arrays for basic biological experimentation.

ACKNOWLEDGMENT

We thank the USDA (TSTAR project HAW00559-04G) for financial support of this work.

Received for review September 9, 2005. Accepted January 26, 2006.

AC051619S

(30) Tsourkas, A.; Behlke, M. A.; Bao, G. *Nucleic Acids Res.* **2002**, *30*, 4208−4215.
(31) Marras, S. A. E.; Kramer, F. R.; Tyagi, S. *Genet. Anal.: Biomol. Eng.* **1999**, *14*, 151−156.
(32) Andronescu, M.; Aguirre-Hernandez, R.; Condon, A.; Hoos, H. H. *Nucleic Acids Res.* **2003**, *31*, 3416−3422.
(33) Bilek, J. Brno University of Technology, Brno, 2001.
(34) Barrettino, D.; Graf, M.; Song, W. H.; Kirstein, K. U.; Hierlemann, A.; Baltes, H. *IEEE J. Solid-State Circuits* **2004**, *39*, 1202−1207.
(35) Weiller, B. H.; Fuqua, P. D.; Osborn, J. V. *J. Electrochem. Soc.* **2004**, *151*, H59−H65.